Fermi National Accelerator Laboratory

FERMILAB-Conf-88/22

QCD: Photo/Hadroproduction of Heavy Flavors; Fermilab E691, E769 & Beyond*

Jeffrey A. Appel
Computing Department
Fermi National Accelerator Laboratory
P.O. Box 500, Batavia, Illinois 60510

February 1988

*Invited talk at the Advanced Research Workshop on QCD Hard Hadronic Processes, St. Croix, U.S. Virgin Islands, October 8-13, 1987.

Operated by Universities Research Association Inc. under contract with the United States Department of Energy

QCD:PHOTO/HADROPRODUCTION OF HEAVY FLAVORS;

FERMILAB E691, E769 & BEYOND

Jeffrey A. Appel

Computing Department
Fermi National Accelerator Laboratory
Batavia, IL. 60510 USA

ABSTRACT

A series of heavy flavor experiments is being performed at the Fermilab Tagged Photon Laboratory. These experiments make use of accurate charged particle tracking, including precise vertex determinations, in an open geometry forward spectrometer. The global transverse energy trigger has high acceptance for all heavy flavor decay modes and allows a wide variety of questions to be addressed.

Some of the results for the completed charm photoproduction experiment (E691), especially production dynamics and relative branching ratios, have been selected for presentation. Their selection is due to their relevance to questions fundamental to QCD, the topic of this workshop. Other results (e.g., on charm particles lifetimes, mixing, Cabibbo single and doubly suppressed decays, etc.) have appeared[1] already or are about to appear.

The current experiment, charm hadroproduction (E769), is also described and its status presented. Finally, plans for future efforts, including beauty hadroproduction, are summarized.

THE TAGGED PHOTON SPECTROMETER

The Tagged Photon Spectrometer (Fig. 1) is by now a fairly standard forward open geometry multiparticle spectrometer.[2] The charged particles are momentum analyzed by a two-magnet system with 35 planes of drift chambers and are identified by use of two, one atmosphere, Cerenkov counters, the first filled with nitrogen and the second with a mixture of 80% helium and 20% nitrogen. An important part of the tracking is performed by 9 planes of 50μm pitch silicon microstrip detectors (SMDs) located just downstream of the target. Electron and photon identification and energy measurements are provided by the electromagnetic calorimeter which, in conjunction with the hadron calorimeter just downstream, measures the neutral and charged hadron energies and positions. One meter of steel absorber precedes a set of 15 muon defining scintillation counters at the downstream end of the experiment. The collaboration which performed E-691 included researchers from the CBPF and the University of Sao Paulo in Brazil, Carleton University, the University of Toronto and the NRC in Canada and from the University of California at Santa Barbara, the University of Colorado and Fermilab in the U.S.[3]

The SMD system contained a total of 6840 readout strips with 50 micron spacing (pitch). The reconstructed interaction vertex had an uncertainty of 20 microns in each transverse direction and about 200 microns along the beam direction. The SMD system has been widely recognized as a crucial part of the improved capability of E691, reducing the background by as much as 2 orders of magnitude relative to previous experience. This reduction comes in two parts essentially. The first element is that by selecting events which have secondary vertices in the fiducial region, one greatly enhances the fraction of charm events in the data sample. Secondly, in calculating effective masses for identifying parent particles, one needs only consider combinations of tracks which come from common vertices downstream of the production vertex. This greatly reduces the number of combinations of tracks tried in searching for charm particles.

A rather beautiful illustration of this occurs in Fig. 2, where a D*D event is reconstructed. One sees the production vertex followed by the downstream decay of the two D^0s in the event. The separation along the beam direction between the initial production point and the first downstream decay is labeled Δz and the ellipses indicate the 1σ resolution of each vertex. If one takes the z axis of the ellipses as uncertainties and divides the Δz by the uncertainty of the separation, one gets what is called $\Delta z/\sigma_z$. By cutting on this parameter, one can get signals for the mass peaks with very little background. Figure 3 shows this for D^0s which decay to $K\pi$ and the even cleaner signals to background when one looks at the events which also have the low energy pion detected for those D^0s which come from D*s.

The improved capability of E691 is a result of more than just the silicon microstrip detectors. Three other features were also important. The first of these is the large quantity of data collected and the possibility of rapidly analyzing the hundred million events. The ACP computer systems was used for a large fraction of the production charged track reconstruction and calorimetry. An equal amount of equivalent Cyber CPU power was also available for physics analysis and some of the

production reconstruction. The total computing power applied to E691 was approximately 300,000 VAX 11/780 equivalent CPU hours.

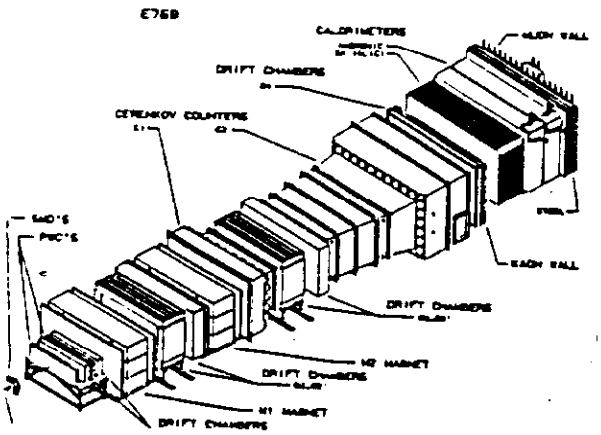

Fig. 1: Schematic View of the Tagged Photon Spectrometer.

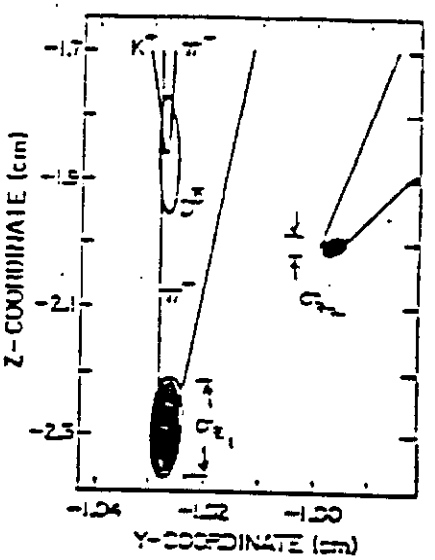

*Fig. 2: Reconstructed D*D Event*

A second additional feature of E691 was running at the Fermilab Tevatron. The accelerator duty factor for data taking was 22 seconds of spill out of a 57 second cycle time, better than 30%. In addition, the higher energy of the Tevatron beam allowed use of higher flux and higher energy secondary beams. Furthermore, the run itself was about 5 months long and the beam was available to the experiment throughout the entire period.

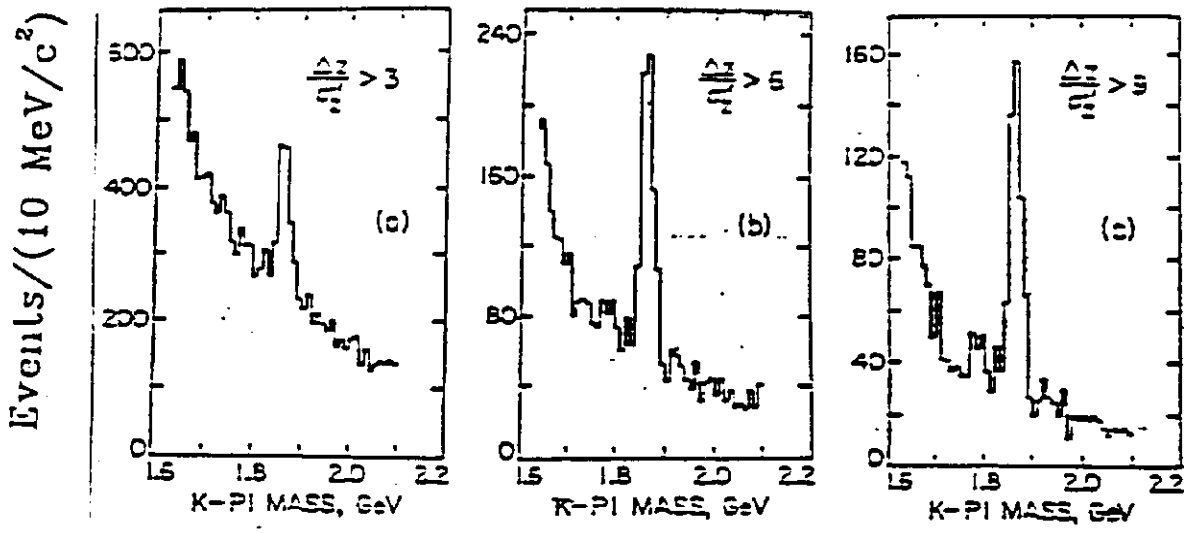

Fig. 3: Mass Distribution of Candidate Kπ Combinations for Three Different Selections of Secondary (the Decay) Vertex Separation from the Production Point.

Finally, the third additional feature in E691 was a global transverse energy trigger.[4] This trigger is based on the simple analog sum of signals from the two calorimeters and provided a rejection factor of about three for non-charm events. The trigger is very open to charm and proved to be about 80% efficient as seen in Fig. 4.

691: PHOTOPRODUCTION OF CHARM

Production Dynamics

The distribution of charm events as a function of global transverse energy (E_t) in the forward hemisphere is the first feature of the production dynamics. This global transverse energy comes largely from the mass of the charm particles produced in pairs. However, it is seen that the forward transverse energy extends to quite high values and is not simply peaked at the threshold value. This is what makes the global E_t trigger work for charm production.

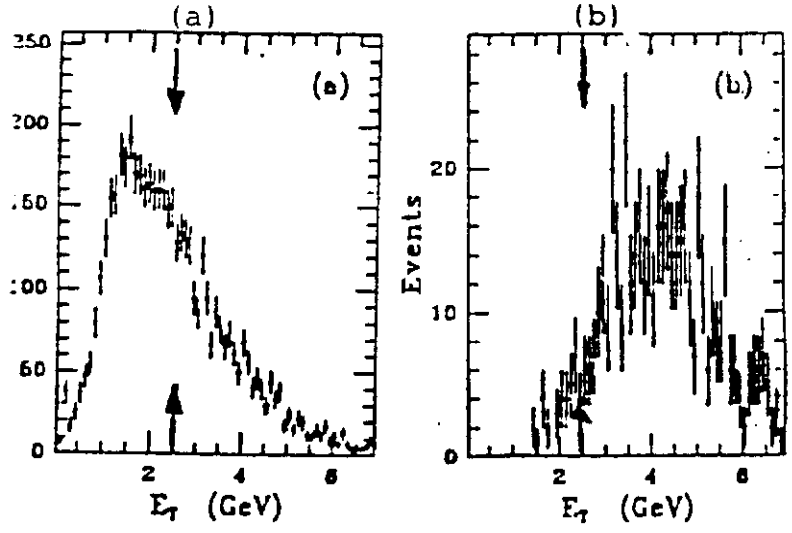

Fig. 4: Global E_T distribution of Events Measured by the Spectrometer (a) for all Hadronic Interactions and (b) for charm events.

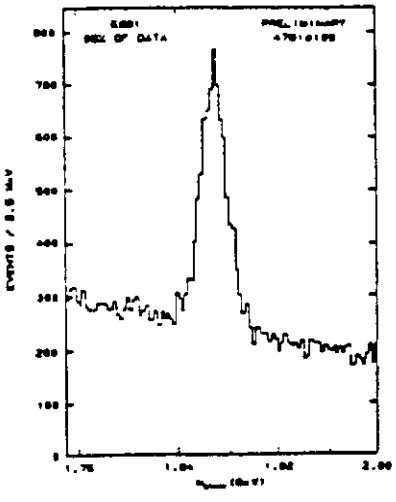

Fig. 5: Effective Mass Distribution of $K\pi\pi$ Combination Candidates for D^+.

Figure 5 shows the sample of charged D^+ used for analysis of the production dynamics. Similar distributions exist for the D^os and D^*s. The data shown here are taken from about 95% of the total data sample and all the results presented are considered preliminary. Distributions of the energy and x_F dependance of D^o and D^+ production are shown in Figs. 6-8 as well as the average P_t^2 of the cross section. Table 1 gives some characterization to this data. We soon expect to have extracted the gluon structure function of the proton from this data assuming a photon gluon fusion model. Thus, there is some check on the internal consistency of the model and we will be reporting more than parameters for an arbitrary fit to the data.

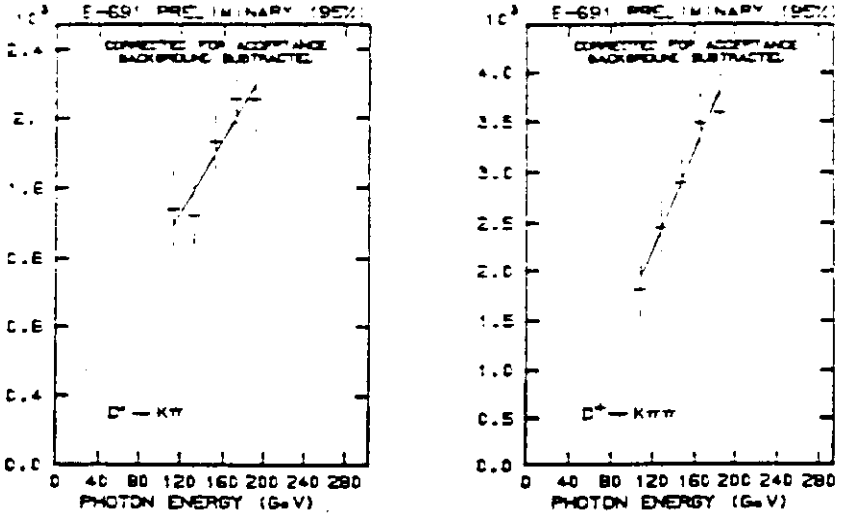

Fig. 6: Energy dependence of photoproduced (a) D^0s and (b) D^+s.

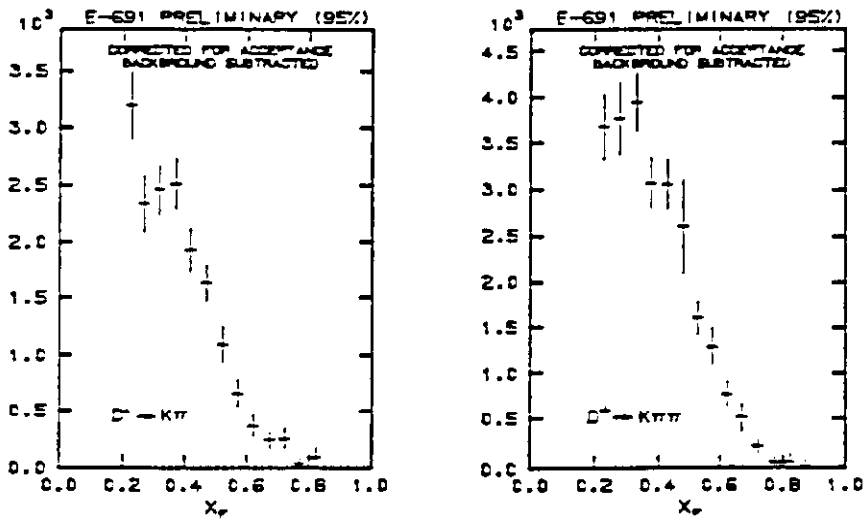

Fig. 7: Feynman x distribution of photoproduced (a) D^0s and (b) D^+s.

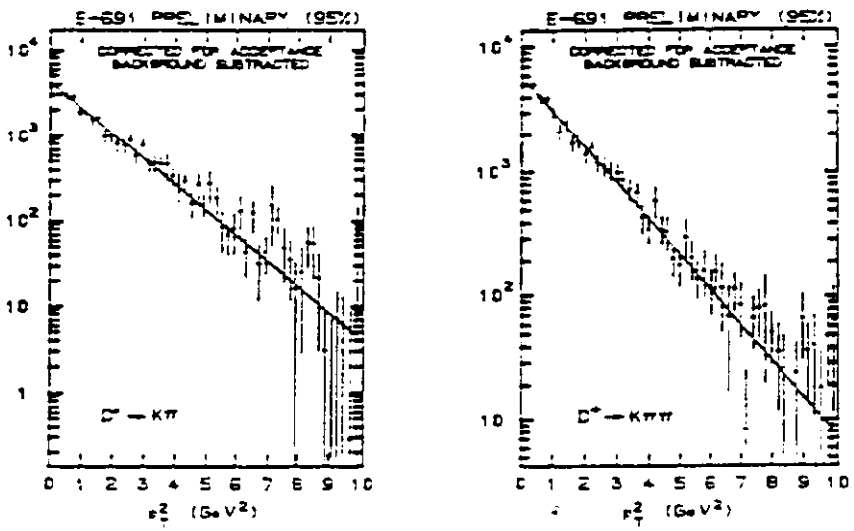

Fig. 8: Transverse momentum distribution of photoproduced (a) D^0s and (b) D^+s.

TABLE 1

Characterization of Photoproduction of D^0s and D^*s*

Characteristic	D^0	D^+
$\sigma(200\ GeV)/\sigma(100\ GeV)$	1.82 ± 0.35	2.46 ± 0.54
n in $(1 - X_F)^n$	2.89 ± 0.12	2.57 ± 0.10
$\langle p_t^2 \rangle$	1.34 ± 0.04	1.43 ± 0.04

**The results shown are preliminary and only the statistical uncertainties are included.*

In our range of 90-260 GeV photon energy, almost equal charm and anti-charm meson production is observed. The associated production seen at lower energies is less than 10% and shows no dependance on the incident photon energy or x_F in the range of 0.2 to 0.6.

Hadronization and Charm Particle Branching Ratios

A fairly consistent picture of charm meson decays is beginning to emerge. This picture explains the unequal lifetimes of the charged and neutral Ds as well as relative rates of the D_s and A_c. Once one has isolated the decay diagrams, we have perhaps an even more isolated quark than in some of the hard QCD processes discussed at this conference. It is a challenge to the theory to describe the hadronization of these isolated quarks. What is the role of such effects as color cancellation, helicity conservation and final state interactions? What is the two body vs. many body and resonant vs. non-resonant nature of the hadronization process?

As an example of the quality of the data which should encourage additional efforts in this area, we examined the $KK\pi$ final state. In Fig. 9 is presented the Dalitz plot of decays corresponding to the charged D and D_s masses. One sees a vertical band corresponding to the ϕ meson and a horizontal band corresponding to K^*. In both cases one also sees the effect of the vector-pseudoscalar nature of the resonant decays. This causes bunching in the relevant band near the edges of the Dalitz plot. All of this can be used to separate the resonant $\phi\pi$ and K^*K decay modes and, after subtraction of the background, also determination of the non-resonant decay of the D meson. Similarly, in the 3π decay made shown in Fig. 10 and in the $KK3\pi$ decay mode shown in Fig. 11, we can separate resonant and non-resonant contributions. The results of all of these data are summarized in Tables 2 and 3. Here we see precision on ratios of branching fractions at the 10-30% level.

TABLE 2

D_s^+ Branching Ratios (B.R) Relative to $B(D_s^+ \to \phi\pi^+)$

Decay Mode	$\frac{B.R.}{B(D_s^+ \to \phi\pi^+)}$
$D_s^+ \to K^{*0}K^+$	0.87 ± 0.13 ± 0.05
$(D_s^+ \to K^-K^+\pi^+)nr$	0.25 ± 0.07 ± 0.05
$D_s^+ \to \phi\pi^+\pi^-\pi^+$	0.42 ± 0.13 ± 0.07
$(D_s^+ \to K^+K^-\pi^+\pi^-\pi^+)nr$	< 0.32 (90% C.L.)

TABLE 3

D^+ Branching Ratios (B.R.) Relative to $B(D^+ \to {}^-\pi^+\pi^+)$ and Absolute Branching Ratios*

Decay Mode	$\frac{B.R.}{B(D^+ \to K^-\pi^+\pi^+)}$	Absolute B.R. (%)
$D^+ \to \phi\pi^+$	0.075±0.008±0.007	0.68±0.07±0.12
$D^+ \to K^{*0}K^+$	0.061±0.009±0.006	0.45±0.08±0.10
$(D^+ \to K^-K^+\pi^+)nr$	0.052±0.008±0.006	0.47±0.07±0.09
$D^+ \to \phi\pi^+\pi^-\pi^+$	< 0.002 (90% C.L.)	< 0.02 (90% C.L.)
$(D^+ \to K^+K^-\pi^+\pi^-\pi^+)nr$	< 0.03 (90% C.L.)	< 0.24 (90% C.L.)

*Using $B(D^+ \to K^-\pi^+\pi^+) = 9.1 \pm 1.4\%$

The isolation of downstream decays allows one to study decay modes which were previously unmeasurable, even in electron-positron storage ring experiments. The 3π final state, in particular, has recently provided the same kind of results as just seen for the states with strange particles in them. Without the silicon microstrip vertexing, one would have had to take combinations of the large numbers of pions produced in final states and the charm states would be swamped by background. Figure 11 shows a significant charged D and D_s signal in the 3π decay mode and an ability to measure the resonant ρ decay state as well. Results are summarized in Table 4.

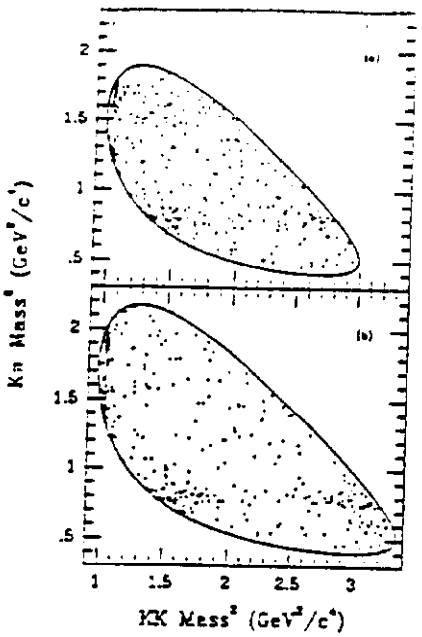

Fig. 4. The Dalitz plots for the (a) D^+ and (b) D_s^+ regions.

Fig. 9: The Dalitz plots for the (a) D^+ and (b) D_S^+ regions.

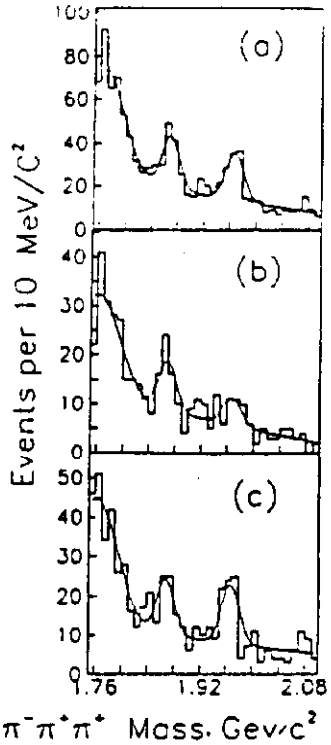

Fig. 10: (a) The $\pi^+\pi^-\pi^+$ mass spectrum for all events passing vertex cuts. The curve represents a fit with linear background, Gaussian peaks for the D^+ and D_S^+, and a peak for the misidentified $D^+ \rightarrow K^-\pi^+\pi^+$ events; (b) The same for events consistent with $\rho^0\pi^+$. (c) The same for events not included in the $\rho^0\pi^+$ sample.

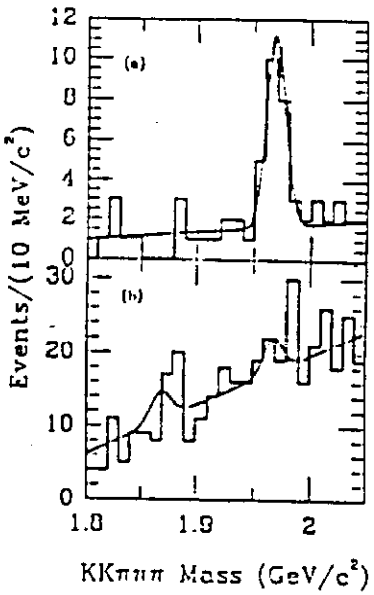

Fig. 11: The $K^+K^-\pi^+\pi^-\pi^+$ mass spectra for the (a) $\phi\pi^+\pi^-\pi^+$ and (b) non-resonant $K^+K^-\pi^+\pi^-\pi^+$ final states.

E769: HADROPRODUCTION OF CHARM

A follow-on experiment, E769, is using a slightly modified tagged photon spectrometer and many of the same techniques to study the hadroproduction of charm particles. The goal of the experiment is to collect about 75,000,000 events for each of the plus and minus beam of tagged pions and kaons. With these, the experiment will study the flavor, A, x, and p_t dependance of charm and charm-strange production. The

experimenters also hope to have larger statistics samples of D_s and Λc relative to E691. This should allow further improvement in lifetime and decay branching ratio information. The collaboration is again composed of physicists[6] from Brazil, Canada and the U.S., but has added Northeastern, Tufts, and Yale Universities and the University of Wisconsin at Madison to make up for the fraction of E691 collaborators who have concentrated their efforts on E691 data analysis and some of whom have moved to other experiments.

TABLE 4

E-691

$\frac{B(D_s^+ \to \pi^+\pi^-\pi^+)}{B(D_s^+ \to \phi\pi^+)}$	=	0.29 ± 0.07 ± 0.05
$\frac{B(D_s^+ \to \rho\pi^+)}{B(D_s^+ \to \phi\pi^+)}$	<	0.08 (90% C.L.)
$\frac{B(D^+ \to \pi^+\pi^-\pi^+)}{B(D^+ \to K^-\pi^+\pi^+)}$	=	0.041 ± 0.008 ± 0.004
$\frac{B(D^+ \to \rho\pi^+)}{B(D^+ \to K^-\pi^+\pi^+)}$	=	0.022 ± 0.008 ± 0.003

The collaboration has made four additions to the E691 apparatus. Given the incident charged beam, it is now possible to include information on this particle in defining vertices. To this end, a 25 micron pitch SMD pair and upstream PWCs of 1mm pitch have been added to the experiment. The target for the incident beam is a set of Be, Al, Cu and W foils with each foil about 200 microns thick. Therefore, primary interactions can be localized better than from the reconstructed tracks alone. The third set of additions is for the downstream tracking where a pair of crossed 25 micron pitch SMDs are added as well as two proportional wire chambers which measure the vertical position upstream of the first magnet. Finally, incident pions and kaons are tagged by Transition Radiation Detector (TRD) and a Differential Isochronous Self-focusing Cerenkov counter (DISC) respectively. The power of these devices to identify incident 250 GeV beam particles is illustrated in Fig. 12. The distributions shown there are only days old, the devices still being tuned for optimum performance. Nevertheless, one can see clean differences in the distributions of signals due to π's, K's and protons in the beam.

This higher beam energy (250 GeV) helps make up for the lower average x of the constituents in the scattering of hadrons relative to the photoproduction scattering. The average photon energy in E691 for charm events was 145 GeV. However, because of the smaller fractional charm production rate with incident hadrons, one can still ask whether E769 will be able to measure the hadroproduction of charm particles. By comparing the features of E769 to E691 we can get some feeling for the confidence felt by the experimenters in their eventual success in this effort. First among these are the extra background suppression tools available in E769.

We have already mentioned the tracking of the incident particle and the use of foil targets which will allow a better determination of the interaction point in E769 relative to E691. Similarly, the 25 micron pitch of the central region of the 4 added SMD planes should help improve the resolution of vertices in the hadroproduction experiment. This will be especially useful in finding Λ_c particles where the lifetime had been measured to be about half that of neutral Ds, for example, and D_ss. The common knowledge on hadroproduction of charm states is that hadroproduction is much harder than photoproduction because of the extra quarks in the event. These eventually become additional particles in the final state which contaminate mass distributions due to the extra combinations in the higher multiplicity events. However, as already pointed out, the use of tracks coming from well defined secondary vertices removes these extra hadrons from the combinations included in mass distributions. Thus the use of SMDs should make hadroproduction much more like photoproduction than was the case before their use.

A major part of the success of E691 was the ability to take a much larger data sample than in previous experimental efforts. This capability has been extended for E769 by an additional factor of more than 3. Furthermore, the data acquisition system (shown in Fig. 13) provides a number of additional useful features. The readout of data in CAMAC has been sped up to 600 nanoseconds per word from the 3 μseconds per word of E691. The CAMAC data is read out in 7 parallel branches relative to 2 in E691. All of this allows more data to be taken into the system and the use of ACP memories allows buffering an entire spill's worth of data. This can then be written to magnetic tape essentially continuously. The tape drives themselves have been upgraded from 75 ips to 100 ips and are written directly from the memories of the ACP modules onto magnetic tape without traversing the internal bus of the general purpose host computer. The experiment is capable of recording greater than 300 events per second with 30% dead time. In E769, the use of ACP processor boards is strictly for event formating and storage, awaiting writing to magnetic tape. No filtering of data has yet been performed in this system although that capability exists.

The use of Smart Crate Controllers (SCCs) and readout buffers (RBUFs) follows an original concept due to Sergio Conetti of McGill University. His designs were re-engineered and extended at Fermilab by Ed Barsotti and Sten Hansen. The software for the system makes use of some general ACP and Computing Department software, but the overall system and most of the specific software in use was written by Steve Bracker and Colin Gay of E769 and Mark Bernett of the Computing Department. The success of this new data acquisition system is indicated by the fact that 1500 full tapes of data have been written in one month with a single day peak of 150 tapes.

BEYOND E769

Assuming that the run which is currently in progress continues to go well, the collaboration anticipates preparing a new proposal. Additional collaborators are also being sought for this effort which will aim at additional charm data and the hadroproduction of beauty. The same

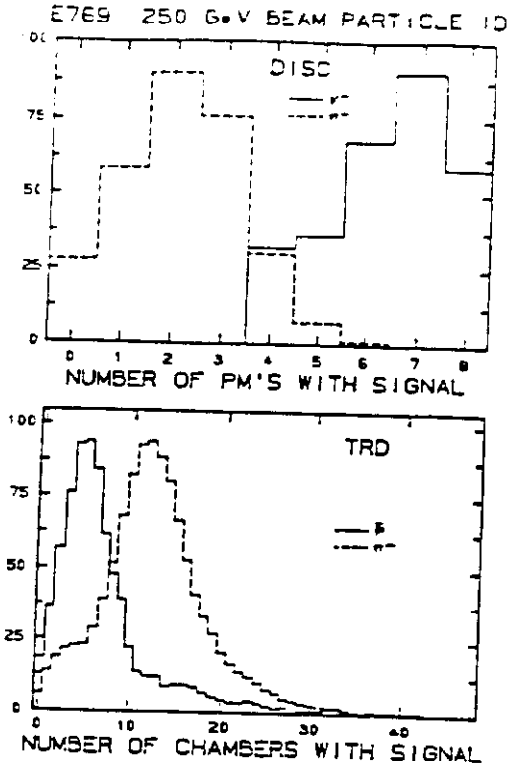

Fig. 12 E769 250 GeV Beam Particle Identification

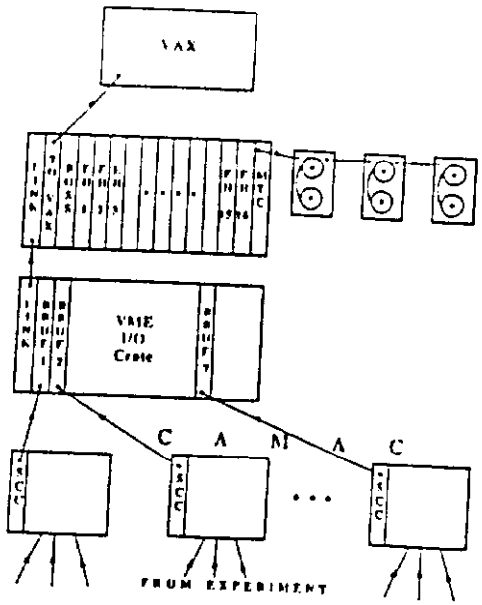

Fig. 13 E769 Data Acquisition System

apparatus and techniques will lie at the heart of the new proposal. However, in order to get to beauty in sufficient quantities, one needs to select events which are a thousand times more rare than the charm particle events. For this, one will increase the incident beam energy and, with it, the beauty cross section. Simply dialing up the threshold on the global transverse energy trigger discriminator from 3 GeV to 10 GeV will provide nearly an order of magnitude of additional rejection. The event readout at that time can be reduced by an additional factor of 2 to 3 which would lead to the need to filter data in the on-line system before writing data to magnetic tape. These features should allow a 1 run experiment to collect on the order of 100 recognizable beauty decays. The use of a hardware trigger for selecting events with multiple decay vertices, high p_t leptons or large multiplicity jumps near the target can increase this and lead to the next generation of beauty physics capabilities.

ACKNOWLEDGMENTS

The author is grateful to all the collaborators on E691 and E769. It is mostly the results of their work which is summarized here. Especially worthy of note in this context are the analyses of Milind Purohit, Audrius Stundzia, Marleigh Sheaff, Lee Lueking, Alice Bean, Paul Karchin, Greg Punkar and Mike Witherell. The research is supported by the U.S. Department of Energy and National Science Foundation, by the Natural Science and Engineering Research Council of Canada, by the National Research Council of Canada, and by the Brazilian Conselho Nacional de Desenvolvimento Cientifico e Technologico.

REFERENCES

1. J.C. Anjos, et al., Phys. Rev. Lett. 58, 311 (1987); Phys. Rev. Lett. 58, 1818 (1987).

2. For details see J. Raab, et al., Fermilab-Pub-87-144, submitted to Phys. Rev. D (1987) and references therein.

3. E-691; University of California-Santa Barbara: A. Bean, T.E. Browder, P.E. Karchin, S. McHugh, R.J. Morrison, G. Punkar, J.R. Raab, M.S. Witherell; Carleton University: P. Estabrooks, J. Pinfold, J.S. Sidhu; Centro Brasileiro de Pesquisas Fisicas: J.C. Anjos, A.F.S. Santoro, M.H.G. Souza; University of Colorado at Boulder: L.E. Cremaldi, J.R. Elliott, M.C. Gibney, U. Nauenberg; Fermi National Accelerator Lab: J.A. Appel, P.M. Mantsch, T. Nash, M.V. Purohit, K. Sliwa, M.D. Sokoloff, W.J. Spalding, M.E. Streetman; National Research Council: M.J. Losty; Universidade de Sao Paulo: C.O. Escobar; University of Toronto: S.B. Bracker, G.F. Hartner, B.R. Kumar, G.J. Luste, J.F. Martin, S.R. Menary, P. Ong, A.B. Stundzia.

4. J.A. Appel, p. 555 in "The Search for Charm, Beauty, and Truth at High Energies," Proc. of a Europhysics Study Conference on High-Energy Physics held November 15-22, 1981, in Erice, Sicily, Italy, G. Bellini and S.C.C. Ting, editors, Plenum Press, New York (1984).

5. E-769; University of California-Santa Barbara: G. Punkar; Centro Brasileiro de Pesquisas Fiscas: G.A. Alves, J.C. Anjos, C. DeBarros, H. DeMotta Filho, A.F.S. Santoro, B. Schulze, M.H.G. Souza; University of Colorado at Boulder: L.M. Cremaldi; Fermilab: J.A. Appel, L. Chen-Tokarek, R. Dixon, H. Fenker, D. Green, L.Lueking, P.M. Mantsch, T. Nash, W.J. Spalding, M.E. Streetman, D. Summers; Institute of Theoretical Physics-Sao Paulo: A. D'Oliveira; Northeastern University: D. Kaplan, I. Leedom, S. Reucroft; University of Toronto: S.B. Bracker, C. Gay, R. Jedicke, G.J. Luste; Tufts University: J. Metheny, R. Milburn, A. Napier; University of Wisconsin at Madison: D. Errede, M. Sheaff; Yale University: P.E. Karchin, Z. Wu.